Backstepping Boundary Stabilization of Linearized 2D Hartman Flow

Chao Xu, Eugenio Schuster, Rafael Vazquez and Miroslav Krstic

***Abstract*— We present a boundary control law that stabilizes the Hartman profile for low magnetic Reynolds numbers in an infinite magnetohydrodynamic (MHD) channel flow. The proposed control law achieves stability in the L^2 norm of the linearized MHD equations, guaranteeing local stability for the fully nonlinear system.**

I. Introduction

A backstepping boundary control law is proposed for stabilization of the 2D linearized magnetohydrodynamic (MHD) channel flow, also known as Hartmann flow. This flow is characterized by an electrically conducting fluid moving between parallel plates in presence of an externally imposed transverse magnetic field. The system is described by the MHD equations, which are a combination of the Navier-Stokes equations and the Maxwell equations.

While control of flows has been an active area for several years now, up until now active feedback flow control developments have had little impact on electrically conducting fluids moving in electromagnetic fields. Prior work in this area focuses mainly on electro-magneto-hydro-dynamic (EMHD) flow control for hydrodynamic drag reduction, through turbulence control, in weak electrically conducting fluids such as saltwater. Traditionally two types of actuator designs have been used: one type generates a Lorentz field parallel to the wall in the streamwise direction, while the other one generates a Lorentz field normal to the wall in the spanwise direction. EMHD flow control has been dominated by strategies that either permanently activate the actuators or pulse them at arbitrary frequencies. However, it has been shown that feedback control schemes, making use of "ideal" sensors, can improve the efficiency, by reducing control power, for both streamwise [1] and spanwise [2], [3] approaches. From a model-based-control point of view, feedback controllers for drag reduction are designed in [4], [5] using distributed control techniques based on linearization and model reduction. Prior work can also be found in the area of mixing enhancement. In [6], a controller, designed using Lyapunov methods, that does not rely on linearization or any type of model reduction is proposed for optimal mixing enhancement by blowing and suction. In [7], the authors investigated optimal perturbations in a magnetohydrodynamic flow bounded by perfectly insulating or conducting walls and the energy growth mechanisms with respect to parameters of the Hartmann flow. The stability of conducting fluids under the presence of a magnetic field was studied extensively in [8] and references therein. The method used in this paper for stabilizing the linearized 2D MHD equations is based on the recently developed backstepping technique for parabolic systems [9], which has already been succesfully applied to the stabilization of 2D and 3D linearized Navier-Stokes channel flows [10], [11].

We organize this paper as follows. In Section II the mathematical model of the MHD channel is stated, the equilibrium profiles are obtained, and the MHD equations are linearized around these equilibrium profiles. Then we convert the linearized MHD equations into the wave-number space by using the Fourier transform technique. This approach allows separate analysis for each wave number, as all pairs are uncoupled from each other. The wave numbers are split into two sets. For the first set, the controlled set, a normal velocity controller is designed in Section III to put the system into a form where a linear Volterra operator, combined with boundary feedback for the tangential velocity, can transform the original normal velocity PDE into a stable heat equation. For the second set, the uncontrolled set, the system is proved to be open loop exponentially stable in Section IV. In addition, the stability of the system is proved for the controlled set of wave numbers. Combining these two results, stability of the closed loop system is proved for all wave numbers in the wave-number space and in the physical space. Section V closes the paper stating the conclusion and the identified future work.

II. Model

A. Governing Equations

We consider the flow of an incompressible, Newtonian (constant viscosity), conducting fluid between parallel plates where an external magnetic field perpendicular to the channel axis is applied. This flow was first investigated experimentally and theoretically by Hartmann [12]. The dimensionless governing equations include the momentum transport equation,

$$\frac{\partial \mathbf{v}}{\partial t} + (\mathbf{v}\cdot\nabla)\mathbf{v} = -\nabla P + \frac{1}{R}\nabla^2\mathbf{v} + N(\mathbf{j}\times\mathbf{B}), \tag{1}$$

and the magnetic induction transport equation,

$$\frac{\partial \mathbf{B}}{\partial t} = \nabla\times(\mathbf{v}\times\mathbf{B}) + \frac{1}{R_m}\nabla^2\mathbf{B}, \tag{2}$$

This work was supported in part by a grant from the Commonwealth of Pennsylvania, Department of Community and Economic Development, through the Pennsylvania Infrastructure Technology Alliance (PITA), and in part by the NSF CAREER award program (ECCS-0645086). C. Xu (chx205@lehigh.edu) and E. Schuster (schuster@lehigh.edu) are with the Department of Mechanical Engineering and Mechanics, Lehigh University, 19 Memorial Drive West, Bethlehem, PA 18015, USA. R. Vazquez, and M. Krstic are with the Department of Mechanical and Aerospace Engineering, University of California at San Diego, La Jolla, CA 92093, USA.

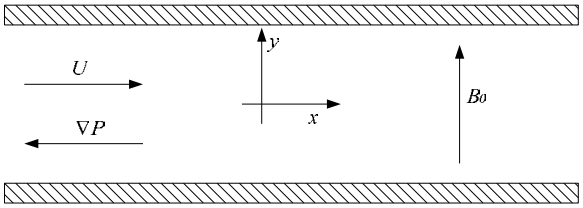

Fig. 1. 2D Hartman flow, $(x, y) \in (-\infty, \infty) \times [0, 1]$.

where $\mathbf{v}$ is the velocity field of the fluid, $\mathbf{B}$ is the magnetic field, $\mathbf{j}$ is the current density, and P is the pressure. R, R_m, and N are the Reynolds number, magnetic Reynolds number, and Stuart (or interaction) number, respectively. The current density is given by Ampere's law, $\mathbf{j} = \frac{1}{R_m}\nabla \times \mathbf{B}$. Both $\mathbf{B}$ and $\mathbf{v}$ are solenoidal, $\nabla \cdot \mathbf{B} = 0, \nabla \cdot \mathbf{v} = 0$. In this work, we consider MHD flow at low magnetic Reynolds number R_m. When $R_m \ll 1$, the induced magnetic filed is very small in comparison with the applied (constant) magnetic field $\mathbf{B}_0$, i.e., $\mathbf{B} \approx \mathbf{B}_0$. Therefore, $\frac{\partial \mathbf{B}}{\partial t} = 0$ in (2). In this case, Ohm's law becomes $\mathbf{j} = -\nabla\phi + \mathbf{v} \times \mathbf{B}_0$, where ϕ is the electric potential. Since $\mathbf{j}$ is a solenoidal field, a Poisson equation is obtained for ϕ by computing the divergence of Ohm's law. The governing equations of the system become

$$\frac{\partial \mathbf{v}}{\partial t} + (\mathbf{v} \cdot \nabla)\mathbf{v} = -\nabla P + \frac{1}{R}\nabla^2\mathbf{v} + N(\mathbf{v} \times \mathbf{B}_0) \times \mathbf{B}_0 - N(\nabla\phi \times \mathbf{B}_0), \quad (3)$$

$$\nabla^2\phi = \nabla \cdot (\mathbf{v} \times \mathbf{B}_0) = \mathbf{B}_0 \cdot \omega, \quad (4)$$

$$\nabla \cdot \mathbf{v} = 0, \quad (5)$$

where $\omega = \nabla \times \mathbf{v}$ is the vorticity. Equations (3)-(5) are referred to as the simplified magnetohydrodynamic equations (SMHD). For the 2-D Hartman flow considered in this work, whose geometrical configuration is illustrated in Fig.1. We write $\mathbf{v}(t, x, y) = U(t, x, y)\hat{\imath} + V(t, x, y)\hat{\jmath}$, $\mathbf{B}_0(t, x, y) = B_0(t, x, y)\hat{\jmath}$ and $P = P(t, x, y)$, then

$$(\mathbf{v} \times \mathbf{B}_0) \times \mathbf{B}_0 = -B_0^2 U\hat{\imath}, \quad (6)$$

$$\nabla\phi \times \mathbf{B}_0 = (\phi_x\hat{\imath} + \phi_y\hat{\jmath}) \times B_0\hat{\jmath} = \phi_x B_0\hat{k}, \quad (7)$$

$$\omega = \nabla \times \mathbf{v} = \left(\frac{\partial V}{\partial x} - \frac{\partial U}{\partial y}\right)\hat{k}, \quad (8)$$

where $\hat{\imath}$, $\hat{\jmath}$ and $\hat{k}$ are the unit vectors of the Euclidean coordinate system employed here. For the last term $\nabla\phi \times \mathbf{B}_0$ in (3), the only component remaining, $\phi_x B_0$, lies in z-direction. Since we consider a 2D geometry,

$$\phi_x(x, y) = 0. \quad (9)$$

Therefore, the Poisson equation (4) for the electric potential $\phi(x, y)$ reduces to a degenerated ordinary differential equation, $\phi_{yy}(x, y) = 0$. Integrating it twice, we obtain

$$\phi(x, y) = C_1(x)y + C_2(x). \quad (10)$$

Differentiating with respect to x, and recalling (9), we obtain $C_1'(x)y + C_2'(x) = 0$, $\forall (x, y) \in (-\infty, \infty) \times [0, 1]$. Evaluating this last expression at $y = 0$ and $y = 1$ respectively, we conclude that C_1 and C_2 must be constants. Assuming non-conducting walls, i.e., $\phi_y|_{y=0,1} = 0$, then we can determine $\phi(x, y)$ as a constant potential field. The SMHD equations (3)-(5) can be written now as

$$U_t + UU_x + VU_y = -P_x + \frac{1}{R}(U_{xx} + U_{yy}) - NB_0^2 U, \quad (11)$$

$$V_t + UV_x + VV_y = -P_y + \frac{1}{R}(V_{xx} + V_{yy}), \quad (12)$$

$$U_x + V_y = 0, \quad (13)$$

with boundary conditions

$$U = 0, \quad V = 0, \text{ at } \Gamma : y = 0, 1, \quad \forall x \in (-\infty, \infty). \quad (14)$$

By differentiating (11) and (12) with respect to x and y, respectively and recalling the incompressibility condition (13), we find a Poisson equation for the pressure $P(t, x, y)$,

$$\nabla^2 P = -2(V_y)^2 - 2V_x U_y - NB_0^2 U_x, \quad (15)$$

with boundary conditions

$$P_y(t, x, 0) = \frac{V_{yy}(t, x, 0)}{R}, \; P_y(t, x, 1) = \frac{V_{yy}(t, x, 1)}{R}. \quad (16)$$

The boundary conditions (16) are obtained by computing (12) at $y = 0, 1$ respectively.

B. Equilibrium Solutions

By recalling the incompressibility condition (13) and assuming the flow fully developed along x-direction, we infer that the equilibrium profile in the y direction, $V^e(x, y)$, satisfies $\partial V^e/\partial y = 0$. Using the boundary condition at the walls (14), we obtain that V^e must be zero. Assuming fully developed and steady conditions, (11) reduces to

$$\frac{1}{R}\frac{\partial^2 U^e}{\partial y^2} - NB_0^2 U^e = \frac{\partial P^e}{\partial x}, \quad (17)$$

and (12) reduces to $\partial P^e/\partial y = 0$. Since the flow is assumed to be fully developed in the x direction, we conclude that $U^e = U^e(y)$, $P^e = P^e(x)$ and $\frac{dP^e}{dx}$ is constant. The solution of equation (17) is given by

$$U^e(y) = A\cosh(\sqrt{RN}B_0 y) + B\sinh(\sqrt{RN}B_0 y) - \frac{\frac{dP^e}{dx}}{NB_0^2}. \quad (18)$$

Using the boundary conditions (14) at the walls we can obtain

$$A = \frac{1}{NB_0^2}\frac{dP^e}{dx}, \quad B = \frac{dP^e}{dx}\frac{1 - \cosh(\sqrt{RN}B_0)}{NB_0^2\sinh(\sqrt{RN}B_0)}. \quad (19)$$

C. Model Linearization

We define the fluctuation variables $u = U - U^e$, $v = V - V^e = V$, $p = P - P^e$, and linearize the SMHD equations (11), (12) and (15) around the equilibrium profile, obtaining a new set of equations given by

$$u_t = \frac{u_{xx} + u_{yy}}{R} - U^e u_x - U_y^e v - p_x - NB_0^2 u, \quad (20)$$

$$v_t = \frac{v_{xx} + v_{yy}}{R} - U^e v_x - p_y, \quad (21)$$

$$p_{xx} + p_{yy} = -2U_y^e v_x - NB_0^2 u_x, \quad (22)$$

with boundary conditions

$$u(x,0)=0, \quad u(x,1)=U_c(x), \tag{23}$$

$$v(x,0)=0, \quad v(x,1)=V_c(x), \tag{24}$$

$$p_y(x,0)=\frac{v_{yy}(x,0)}{R}, \tag{25}$$

$$p_y(x,1)=\frac{v_{yy}(x,1)+(V_c)_{xx}(x)}{R}-(V_c)_t(x), \tag{26}$$

where $U_c(t,x,1)$ and $V_c(t,x,1)$ are the tangential and normal control laws implemented at the boundary $y=1$, which are to be designed in the following section. Boundary conditions (25) and (26) are obtained by evaluating (21) at the boundaries. The continuity equation (13) is still verified

$$u_x+v_y=0. \tag{27}$$

We use the Fourier transform on x-direction, defined as

$$f(k,y)=\int_{-\infty}^{\infty}f(x,y)e^{-2\pi ikx}dx,\ f(x,y)=\int_{-\infty}^{\infty}f(k,y)e^{2\pi ikx}dk, \tag{28}$$

to transform the system equations to frequency domain. Note that we use the same symbol f for both the original $f(x,y)$ and the tranformed $f(k,y)$. In the transform pair (28), k is called the wave number. The linearized model (20)-(22) written in the wave number domain is

$$u_t=\frac{u_{yy}-4k^2\pi^2u}{R}-2k\pi i(U^eu+p)-U_y^ev-NB_0^2u, \tag{29}$$

$$v_t=\frac{-4k^2\pi^2v+v_{yy}}{R}-2k\pi iU^ev-p_y, \tag{30}$$

$$p_{yy}=4k^2\pi^2p-4k\pi iU_y^ev-2k\pi iNB_0^2u, \tag{31}$$

with boundary conditions

$$u(k,0)=0, \quad u(k,1)=U_c(k), \tag{32}$$

$$v(k,0)=0, \quad v(k,1)=V_c(k), \tag{33}$$

$$p_y(k,0)=\frac{v_{yy}(k,0)}{R}, \tag{34}$$

$$p_y(k,1)=\frac{v_{yy}(k,1)-4\pi^2k^2(V_c)(k)}{R}-(V_c)_t(k), \tag{35}$$

where U_c, V_c are the Fourier transforms of the to-be-designed tangential and normal control laws at the boundary $y=1$. The continuity equation (13) is transformed into the following form

$$2\pi kiu(k,y)+v_y(k,y)=0. \tag{36}$$

One of the properties of the Fourier transform, called Parseval's theorem, states that the L^2 norm in Fourier space is equal to the L^2 norm in physical space, i.e.,

$$\|f\|_{L^2}^2=\int_0^1\int_{-\infty}^{\infty}f^2(k,y)dkdy=\int_0^1\int_{-\infty}^{\infty}f^2(x,y)dxdy. \tag{37}$$

In Section IV, we will use this property to derive L^2 exponential stability in physical space from the same property in Fourier space. We also define the norm of $f(k,y)$ with respect to y as $\|f(k)\|_{\hat{L}^2}^2=\int_0^1|f(k,y)|^2dy$. The relationship between the $\hat{L}_2$ norm and the L^2 norm is given by $\|f\|_{L^2}^2=\int_{-\infty}^{\infty}\|f(k)\|_{\hat{L}^2}^2dk$.

III. Controller Design

It is a well-known fact [13] that there exist two wave-number bounds m and M for which the the system (29)-(36) is exponentially stable without any external control in the range $|k|\geq M$ and $|k|\leq m$. By a proper design of the control laws $U_c(k)$ and $V_c(k)$ in this section, we stabilize the system for wave numbers in the range $m<|k|<M$. The bounds m and M are estimated by the Lyapunov method in Section IV-A. We separate the controlled and uncontrolled sets mathematically using the following function

$$\chi(k)=\begin{cases}1, & m<|k|<M\\ 0, & \text{otherwise.}\end{cases} \tag{38}$$

The transformed Poisson equation for the pressure (31) is an inhomogenous ordinary differential equation in Fourier space. Its solution can be obtained via the coefficient variation approach as follows,

$$\begin{aligned}p(k,y)=&\int_0^y\left(2iU_\xi^ev+iNB_0^2u\right)\sinh[2k\pi(\xi-y)]d\xi\\&+c_1\cosh(2k\pi y)+c_2\sinh(2k\pi y).\end{aligned} \tag{39}$$

Applying the boundary conditions (34) and (35) we can obtain

$$c_2=\frac{v_{yy}(k,0)}{2k\pi R}, \tag{40}$$

$$\begin{aligned}c_1=&\frac{v_{yy}(k,1)-4\pi^2k^2(V_c)(k)}{2k\pi R\sinh 2k\pi}-\frac{(V_c)_t(k)}{2k\pi\sinh 2k\pi}\\&-\frac{v_{yy}(k,0)}{2k\pi R\sinh 2k\pi}\cosh 2k\pi\\&+\int_0^1\frac{\cosh[2k\pi(\xi-1)]}{\sinh 2k\pi}\left(2iU_\xi^ev+iNB_0^2u\right)d\xi.\end{aligned} \tag{41}$$

Substituting $p(k,y)$ into equation (29) we finally rewrite (29) as (44) (see the top of next page), with boundary conditions

$$u(k,0)=0, \quad u(k,1)=U_c(k). \tag{42}$$

We do not need to rewrite and control the v equation (30) because using the continuity equation (36) and the fact that $v(k,0)=0$, we can write v in terms of u

$$v(k,y)=\int_0^y v_y(k,\eta)d\eta=-2k\pi i\int_0^y u(k,\eta)d\eta. \tag{43}$$

Thus, if u is stabilized, this dependence means that v is also stabilized. We now design the controllers in two steps. For the first step we define

$$\begin{aligned}(V_c)_t=&2k\pi i\int_0^1\{2U_\xi^e\cosh[2k\pi(\xi-1)]\\&+iNB_0^2\sinh[2k\pi(1-\xi)]\}v(k,\xi)d\xi-NB_0^2V_c(k)\\&+\frac{2k\pi i\left[u_y(k,0)-u_y(k,1)\right]-4k^2\pi^2V_c(k)}{R},\end{aligned} \tag{45}$$

so that (44) has a strict-feedback form [9]. Introducing the feedback law (45) into (44) leads to

$$u_t=\frac{u_{yy}-4k^2\pi^2u}{R}+\lambda(k,y)u+g(k,y)u_y(k,0)+\int_0^y f(k,y,\xi)ud\xi, \tag{46}$$

$$u_t = \frac{-4k^2\pi^2 u + u_{yy}}{R} - 2k\pi i U^e u - NB_0^2 u + 2k\pi i U_y^e \int_0^y u(k,\eta)d\eta + 8k^2\pi^2 i \int_0^y \left\{ \int_\xi^y U_\eta^e \sinh[2k\pi(y-\eta)]d\eta \right\} u(k,\xi)d\xi$$
$$- 2k\pi NB_0^2 \int_0^y \sinh[2k\pi(y-\xi)]u(k,\xi)d\xi + 2k\pi \frac{\cosh(2k\pi(y-1))}{\sinh 2k\pi} \frac{u_y(k,0)}{R}$$
$$+ 2k\pi \frac{\cosh 2k\pi y}{\sinh 2k\pi} \int_0^1 \left\{ 2\cosh 2k\pi(\xi-1) U_\xi^e + iNB_0^2 \sinh[2k\pi(1-\xi)] \right\} v(k,\xi)d\xi + iNB_0^2 \frac{\cosh 2k\pi y}{\sinh 2k\pi} V_c(k)$$
$$+ i \frac{\cosh 2k\pi y}{\sinh 2k\pi} \left(\frac{2k\pi i u_y(k,1) + 4k^2\pi^2 V_c(k)}{R} + (V_c)_t(k) \right) \tag{44}$$

where

$$\lambda(k,y) = -\left(2k\pi i U^e + NB_0^2\right), \tag{47}$$
$$g(k,y) = \frac{2k\pi}{R} \frac{\cosh[2k\pi(y-1)] - \cosh(2k\pi y)}{\sinh 2k\pi}, \tag{48}$$
$$f(k,y,\xi) = 8k^2\pi^2 i \int_\xi^y U_\eta^e \sinh[2k\pi(y-\eta)]d\eta + 2k\pi i U_y^e - 2k\pi NB_0^2 \sinh[2k\pi(y-\xi)]. \tag{49}$$

For the second step we note that (46) is a parabolic partial integro-differential equation and can be stabilized using the backstepping technique recently introduced in [9]. We define a backstepping tranformation,

$$\alpha = u - \int_0^y K(k,y,\eta)u(t,k,\eta)d\eta, \tag{50}$$

that maps, for each wave number $k \in (m, M)$, the equation for u (46) into a heat equation

$$\alpha_t = \frac{1}{R}(\alpha_{yy} - 4k^2\pi^2\alpha), \tag{51}$$
$$\alpha(k,0) = 0, \quad \alpha(k,1) = 0. \tag{52}$$

The inverse backstepping transformation is defined as

$$u = \alpha + \int_0^y L(k,y,\eta)\alpha(t,k,\eta)d\eta. \tag{53}$$

By differentiating (50) with respect to t and y (twice), and then by substituting the obtained derivatives into (51), we arrive at the following PDEs and boundary conditions for the kernel $K(y,\eta)$, in the domain $\mathcal{D} = \{(y,\eta)|0 \le \eta \le y \le 1\}$,

$$\frac{1}{R}\left[K_{yy}(y,\eta) - K_{\eta\eta}(y,\eta)\right] = \lambda(\eta)K(y,\eta) - f(y,\eta) + \int_\eta^y K(y,\xi)f(\xi,\eta)d\xi, \tag{54}$$

with boundary conditions

$$\frac{2}{R}\frac{dK(y,y)}{dy} = -\lambda(y), \tag{55}$$
$$\frac{1}{R}K(y,0) = -g(y) + \int_0^y K(y,\eta)g(\eta)d\eta. \tag{56}$$

We evaluate the backstepping transform (50) at the boundary $y = 1$ to obtain

$$\alpha(k,1) = u(k,1) - \int_0^1 K(k,1,\eta)u(t,k,\eta)d\eta. \tag{57}$$

Then we substitute (42) and (52) into (57) to obtain the tangential control law

$$U_c = \int_0^1 K(k,1,\eta)u(t,k,\eta)d\eta. \tag{58}$$

Similarly, the equation for the inverse kernel L defined in (53) is

$$\frac{1}{R}\left[L_{yy}(y,\eta) - L_{\eta\eta}(y,\eta)\right] = -\lambda(\eta)L(y,\eta) - f(y,\eta) - \int_\eta^y L(y,\xi)f(\xi,\eta)d\xi d\eta \tag{59}$$

with boundary conditions

$$\frac{2}{R}\frac{dL(y,y)}{dy} = -\lambda(y), \tag{60}$$
$$\frac{1}{R}L(y,0) = -g(y). \tag{61}$$

It can be proved that both K and L equations have smooth solutions. Equations (54)-(56) and (59)-(61) can be solved either numerically or symbolically by using an equivalent integral equation formulation (that can be solved via a successive approximation series [9]). We now convert the control laws (45) and (58) back to the physical space via inverse Fourier transform,

$$U_c(t,x) = \int_0^1 \int_{-\infty}^{\infty} Q_u(x-\xi,\eta)u(t,\xi,\eta)d\xi d\eta, \tag{62}$$
$$V_c(t,x) = h(t,x), \tag{63}$$

where h verifies the parabolic equation

$$h_t = \frac{1}{R}h_{xx} - NB_0^2 h(t,x) + l(t,x), \tag{64}$$

where the function $l(t,x)$ is given by

$$l(t,x) = \int_0^1 \int_{-\infty}^{\infty} Q_v(x-\xi,\eta)v(t,\xi,\eta)d\xi d\eta + \int_{-\infty}^{\infty} Q_0(x-\xi)\left[u_y(t,\xi,0) - u_y(t,\xi,1)\right]d\xi, \tag{65}$$

and the kernel Q_u, Q_v, and Q_0 are defined as,

$$Q_u(x-\xi,\eta) = \int_{-\infty}^{\infty} \chi(k)K(k,1,\eta)e^{(2k\pi i(x-\xi))}dk, \tag{66}$$
$$Q_v(x-\xi,\eta) = \int_{-\infty}^{\infty} \chi(k)2k\pi i\{2U_\eta^e \cosh[2k\pi(\eta-1)] + iNB_0^2 \sinh[2k\pi(1-\eta)]\}e^{(2k\pi i(x-\xi))}dk, \tag{67}$$
$$Q_0(x-\xi) = \int_{-\infty}^{\infty} \chi(k)\frac{2k\pi i}{R}e^{(2k\pi i(x-\xi))}dk, \tag{68}$$

and $\chi(k)$ is defined in (38). The stable parabolic equation (64) determines the dynamics of the tangential controller. Due to the compatibility conditions, we let $h(0,x) = v(t,x,y)|_{t=0,y=1}$ as the initial condition.

IV. Stability Analysis

In Section III, we have derived control laws for both the normal and the tangential directions at the boundary $y=1$. We state our main result at the beginning of this section. In Fourier space, we prove the stability of the uncontrolled set of wave numbers as a first step, and the stability of the controlled set of wave numbers as a second step. Finally, we use these results to prove Theorem 1.

Theorem 1: For the linearized system (20)-(26) with the feedback laws (62) and (63), the equilibrium profile $u(t,x,y) = v(t,x,y) = 0$ is exponentially stable in the L^2 sense:

$$\|u(t)\|_{L^2}^2+\|v(t)\|_{L^2}^2 \leq C_0 e^{\frac{-\pi^2 t}{R}} \left(\|u(0)\|_{L^2}^2+\|v(0)\|_{L^2}^2\right), \quad (69)$$

where C_0 is defined as

$$C_0=(1+4\pi^2M^2) \max_{k\in(m,M)} \{(1+\|L\|_\infty)^2(1+\|K\|_\infty)^2\}, \quad (70)$$

and the norm $\|\cdot\|_\infty$ is defined as $\|f\|_\infty = \max|f(y,\eta)|$.

A. Uncontrolled Wave Number Analysis

For the uncontrolled system (29)-(30), we define the Lyapunov functional for each wave number k as

$$E(t) = \frac{1}{2}\int_0^1 (u\bar{u}+v\bar{v})dy, \quad (71)$$

where $\bar{u}$ and $\bar{v}$ denote the complex conjugates of u and v, respectively. The time derivative of E is

$$\begin{aligned}\frac{dE(t)}{dt} &= \int_0^1 \frac{-4k^2\pi^2}{R}(u\bar{u}+v\bar{v})dy - \int_0^1 U_y^e \frac{u\bar{v}+\bar{u}v}{2}dy \\ &\quad - \frac{1}{R}\int_0^1 (u_y\bar{u}_y+v_y\bar{v}_y)dy - \int_0^1 NB_0^2 u\bar{u}dy. \end{aligned} \quad (72)$$

Since N, the Stuart number, is positive, then we have

$$\begin{aligned}\frac{dE(t)}{dt} &\leq \frac{-8k^2\pi^2}{R}\frac{1}{2}\int_0^1 (u\bar{u}+v\bar{v})dy \\ &\quad - \frac{1}{R}\int_0^1 (u_y\bar{u}_y+v_y\bar{v}_y)dy + \int_0^1 \left(-U_y^e\right)\frac{u\bar{v}+\bar{u}v}{2}dy. \end{aligned} \quad (73)$$

We state now the following lemma without proof:

Lemma 2 (Poincaré Inequality [14]): Given $f \in H$, where

$$H = \left\{f \in C^0([0,1]) | f(0) = f(1) = 0\right\}, \quad (74)$$

with f' piecewise continuous, then $\|f\| \leq \frac{1}{\pi}\|f'\|$, where $\|f\|$ is given by $\|f\|^2 = \int_0^1 |f(x)|^2 dx$.

Using the Poincaré inequality we can obtain a bound for the second term in (73), i.e.,

$$\pi^2 \int_0^1 (u\bar{u}+v\bar{v})dy \leq \int_0^1 (u_y\bar{u}_y+v_y\bar{v}_y)dy. \quad (75)$$

For the third term in (73), we note that (18), i.e., $U^e(y)$, is a "parabola-like" symmetric equilibrium profile with respect to the axis $y=\frac{1}{2}$, then we can obtain $|U_y^e| < U_y^e(0) = -U_y^e(1)$. Additionally, we have the following bound estimate

$$\frac{u\bar{v}+\bar{u}v}{2} = \Re(u\bar{v}) \leq |u\bar{v}| = |u||v| \leq \frac{|u|^2+|v|^2}{2}. \quad (76)$$

Therefore, taking into account (71), (75), and (76) (together with the bound for $|U_y^e|$) we can bound the time derivative of $E(t)$ in (73) as

$$\frac{dE(t)}{dt} \leq \left[\frac{-8k^2\pi^2}{R} - \frac{2\pi^2}{R} + \frac{dU^e(0)}{dy}\right] E(t). \quad (77)$$

Proposition 3: For the linearized system (29)-(35), if $m = \frac{\pi}{4RdU^e(0)/dy}$, and $M = \frac{1}{2\pi}\sqrt{\frac{R}{2}\frac{dU^e(0)}{dy}}$, then for both $|k| \leq m$ and $|k| \geq M$, the equilibrium $u = v = 0$ of the uncontrolled system is exponentially stable in the L^2 sense,

$$\|v(t,k)\|_{\hat{L}^2}^2+\|u(t,k)\|_{\hat{L}^2}^2 \leq e^{\frac{-\pi^2 t}{R}}\left(\|v(0,k)\|_{\hat{L}^2}^2+\|u(0,k)\|_{\hat{L}^2}^2\right). \quad (78)$$

Proof: If $|k| \geq \frac{1}{2\pi}\sqrt{\frac{R}{2}\frac{dU^e(0)}{dy}}$, we have

$$\frac{dE(t)}{dt} \leq -\frac{2\pi^2}{R}E(t). \quad (79)$$

Additionally, by using the continuity equation (43) we can bound (73) as

$$\frac{dE(t)}{dt} \leq \left[\frac{-8k^2\pi^2}{R} - \frac{2\pi^2}{R} + 4|k|\pi\frac{dU^e(0)}{dy}\right] E(t). \quad (80)$$

Thus, if $|k| \leq \frac{\pi}{4RdU^e(0)/dy}$, then $\frac{dE(t)}{dt} \leq -\frac{\pi^2}{R}E(t)$. Taking into account the two bounds obtained for $\frac{dE(t)}{dt}$ and the definition (71), we can prove this proposition. ■

In the physical space we can get similar stability property via the Parseval's theorem:

Proposition 4: The variables $\epsilon_u(t,x,y)$ and $\epsilon_v(t,x,y)$, defined as

$$\epsilon_u(t,x,y) = \int_{-\infty}^{\infty}(1-\chi(k))u(t,k,y)e^{2k\pi ix}dk, \quad (81)$$

$$\epsilon_v(t,x,y) = \int_{-\infty}^{\infty}(1-\chi(k))v(t,k,y)e^{2k\pi ix}dk, \quad (82)$$

decay exponentially in the L^2 sense:

$$\|\epsilon_u(t)\|_{L^2}^2+\|\epsilon_v(t)\|_{L^2}^2 \leq e^{\frac{-\pi^2 t}{R}}\left(\|\epsilon_u(0)\|_{L^2}^2+\|\epsilon_v(0)\|_{L^2}^2\right). \quad (83)$$

Proof: Combining Proposition 3 and Parseval's theorem (37) we can prove this proposition. ■

B. Controlled Wave Number Analysis

In this subsection, we prove the exponential stability of the linearized system with feedback control, not only in Fourier space but also in physical space, for the controlled set of wave numbers.

Proposition 5: For any wave number $|k| \in (m,M)$, the equilibrium $u = v = 0$ of the system (29)-(35) with feedback control laws (45), (58) is exponentially stable in the L^2 sense,

$$\|v(t)\|_{\hat{L}^2}^2+\|u(t)\|_{\hat{L}^2}^2 \leq C_0 e^{\frac{-2\pi^2 t}{R}}\left(\|v(0)\|_{\hat{L}^2}^2+\|u(0)\|_{\hat{L}^2}^2\right). \quad (84)$$

Proof: For the heat equation (51), we can compute

$$\|\alpha(t,k)\|^2_{\hat{L}^2} = \int_0^1 \alpha(t,k,y)\bar{\alpha}(t,k,y)dy, \tag{85}$$

with the time derivative

$$\frac{d\|\alpha(t,k)\|^2_{\hat{L}^2}}{dt} \leq -\frac{2\pi^2}{R}\int_0^1 \alpha\bar{\alpha}dy. \tag{86}$$

Then, using Gronwall's inequality [14], we obtain

$$\|\alpha(t,k)\|^2_{\hat{L}^2} \leq e^{-\frac{2\pi^2 t}{R}}\|\alpha(0,k)\|^2_{\hat{L}^2}. \tag{87}$$

By using (43), (50) and (53), we obtain

$$\alpha = i\frac{v_y - \int_0^y K(y,\eta)v_y(t,\eta)d\eta}{2k\pi}, \tag{88}$$

$$v = -2k\pi i\int_0^y \left[1 + \int_\eta^y L(\eta,\xi)d\xi\right]\alpha(t,\eta)d\eta. \tag{89}$$

By using (53) and (89), we can obtain a bound for $\left(\|u(t,k)\|^2_{\hat{L}^2} + \|v(t,k)\|^2_{\hat{L}^2}\right)$ in terms of $\|\alpha(0,k)\|^2_{\hat{L}^2}$, i.e.,

$$\begin{aligned}
&\|u(t,k)\|^2_{\hat{L}^2} + \|v(t,k)\|^2_{\hat{L}^2} \\
&\leq \int_0^1 (1+\|L\|_\infty)^2|\alpha|^2dy + 4k^2\pi^2\int_0^1(1+\|L\|_\infty)^2|\alpha|^2dy \\
&\leq (1+4M^2\pi^2)(1+\|L\|_\infty)^2 e^{-\frac{2\pi^2 t}{R}}\|\alpha(0,k)\|^2_{\hat{L}^2}.
\end{aligned} \tag{90}$$

Recalling (50) as follows

$$\begin{aligned}
\|\alpha(0,k)\|^2_{\hat{L}^2} &= \int_0^1 \left|u - \int_0^y K(y,\eta)u(0,\eta)\right|^2 d\eta \\
&\leq (1+\|K\|_\infty)^2\left(\|u(0,k)\|^2_{\hat{L}^2} + \|v(0,k)\|^2_{\hat{L}^2}\right).
\end{aligned} \tag{91}$$

Combing (90) and (91), we finish the proof. ■

Proposition 6: Defining

$$u^*(t,x,y) = \int_{-\infty}^{\infty}\chi(k)u(t,k,y)e^{2k\pi ix}dk, \tag{92}$$

$$v^*(t,x,y) = \int_{-\infty}^{\infty}\chi(k)v(t,k,y)e^{2k\pi ix}dk, \tag{93}$$

for the linearized system (20)-(26) with the feedback laws (62) and (63), the variables $u^*(t,x,y)$ and $v^*(t,x,y)$ decay exponentially:

$$\begin{aligned}
&\|u^*(t)\|^2_{L^2} + \|v^*(t)\|^2_{L^2} \\
&\leq C_0 e^{-\frac{2\pi^2}{R}t}\left(\|u^*(0)\|^2_{L^2} + \|v^*(0)\|^2_{L^2}\right).
\end{aligned} \tag{94}$$

Proof: Combining Proposition 5 and the Parseval's theorem (37), we can prove this proposition. ■

Finally, by using Proposition 4 and 6 we can prove exponential stability of the linear system (20)-(26) over the entire wave number range, and therefore finish the proof for Theorem 1.

V. Conclusions and Future Work

We have designed backstepping-based boundary feedback controllers which exponentially stabilize the 2D magnetohydrodynamic equations linearized around a Hartmann equilibrium profile in the L^2 sense. The results have been presented in 2D for ease of notation. Since 3D channels are spatially invariant in both streamwise and spanwise direction, the design can be extended to 3D by applying the Fourier transform in both invariant directions and following similar steps. It is also worth to mentioning that the design can be extended to periodic channel flow, both in 2D and 3D, by substituting the Fourier transform by a Fourier series. The controllers derived in this work are written as state feedback. An observer has been developed based on [15], and has been presented in [16].

Acknowledgement

We thank Jennie Cochran for helpful discussions and for reviewing the paper.

References

[1] E. Spong, J. Reizes, and E. Leonardi, "Efficiency improvements of electromagnetic flow control," *Heat and Fluid Flow*, vol. 26, pp. 635–655, 2005.

[2] H. Choi, P. Moin, and J. Kim, "Active turbulence control for drag reduction in wall-bounded flows," *J. Fluid. Mech.*, vol. 262, pp. 75–110, 1994.

[3] T. Berger, J. Kim, C. Lee, and J. Lim, "Turbulent boundary layer control utilizing the Lorentz force," *Phys. Fluids*, vol. 12, pp. 631–649, 2000.

[4] J. Baker, A. Armaou, and P. Christofides, "Drag reduction in transitional linearized channel flow using distributed control," *Int. J. Control*, vol. 75, no. 15, pp. 1213–1218, 2002.

[5] S. Singh and P. Bandyopadhyay, "Linear feedback control of boundary layer using electromagnetic microtiles," *Transactions of ASME*, vol. 119, pp. 852–858, 1997.

[6] E. Schuster and M. Krstic, "Inverse optimal boundary control for mixing in magnetohydrodynamic channel flows," *42th IEEE Conference on Decision and Control*, 2003.

[7] C. Airau and M. Castets, "On the amplification of small disturbances in a channel flow with a normal magnetic field," *Physics of Fluids*, vol. 16, pp. 2991–3005, Aug. 2004.

[8] V. Vladimirov and K. Ilin, "The three-dimensional stability of steady magnetohydrodynamic flows of an ideal fluid," *Physics of Plasmas*, vol. 5, no. 12, pp. 4199–204, 1998.

[9] A. Smyshlyaev and M. Krstic, "Closed form boundary state feedbacks for a class of partial integro-differential equations," *IEEE Transactions on Automatic Control*, vol. 49, pp. 2185–2202, 2004.

[10] R. Vazquez and M. Krstic, "A closed-form feedback controller for stabilization of linearized Navier-Stokes equations: the 2D Poisseuille flow," *45th IEEE Conference on Decision and Control*, 2005.

[11] J. Cochran, R. Vazquez, and M. Krstic, "Backstepping boundary control of Navier-Stokes channel flow: A 3D extension," *2006 American Control Conference*, 2006.

[12] J. Hartmann, "Theory of the laminar flow of an electrically conductive liquid in a homogeneous magnetic field," *Det Kgl. Danske Videnskabernes Selskab. Mathematisk-fysiske Meddelelser*, vol. XV (6), pp. 1–27.

[13] P. Schmid and D. Henningson, *Stability and Transition in Shear Flows*. New York: Springer, 2001.

[14] A. Tveito and R. Winther, *Introduction to Partial Differential Equations: A Computational Approach, (Texts in Applied Mathematics 29)*. New York: Springer-Verlag, 1998.

[15] A. Smyshlyaev and M. Krstic, "Backstepping observers for parabolic PDEs," *Systems and Control Letters*, vol. 54, pp. 1953–1971, 2005.

[16] R. Vazquez, E. Schuster, and M. Krstic, "A closed-form observer for the 3D inductionless MHD and Navier-Stokes channel flow," *46th IEEE Conference on Decision and Control*, 2006.